The effect of injector barrier thickness and doping level on current transport and optical transition width in a λ~8.0 μm quantum cascade structure

Scott S. Howard,[1,a)] Daniel P. Howard,[1,2] Kale Franz,[1] Anthony Hoffman,[1] Deborah L. Sivco,[3] and Claire F. Gmachl[1]
[1]*Department of Electrical Engineering, Princeton University, Princeton, New Jersey 08544, USA*
[2]*University of Dayton, Dayton, Ohio 45469, USA*
[3]*Alcatel-Lucent, Murray Hill, New Jersey 07974, USA*

(Received 7 June 2008; accepted 27 October 2008; published online 12 November 2008)

We experimentally study the optical transition width and current transport properties of a set of λ~8.0 μm quantum cascade (QC) structures with varying injector barrier thickness and doping level. For this high-performance QC laser structure, a 50% reduction in doping level and a 33% reduction in injection barrier thickness yield five times stronger luminescence, 20% smaller optical transition linewidth, and improved current-voltage characteristics. These results demonstrate how high-performance QC laser structures can be engineered to produce narrow gain spectra at and above room temperature. © *2008 American Institute of Physics*. [DOI: 10.1063/1.3028013]

Improved midinfrared quantum cascade (QC) laser performance has been accomplished by innovations both in conduction band design[1] and fabrication.[2] Continued improvements in design require a detailed understanding of all factors that influence the temperature dependent gain. The optical transition width is a frequently overlooked component of the gain because it is often ascribed to material and interface quality alone. In this study, we examine the optical transition width as a function of two design parameters—the injector barrier thickness and injector doping level.

Optical gain is inversely proportional to the optical transition width $2\gamma_{32}$. In semiconductor diode lasers, the broadening of the transition is due to the opposite sign of the effective mass of electrons and holes, causing a wide range of allowable energy transitions. The minibands of QC lasers, however, can be considered almost parallel in energy-momentum (E-k) space so that intersubband transition broadening is not due to electron dispersion. A λ~8.0 μm QC laser has a photon energy of about 155 meV and a typical optical transition width of approximately 15 meV, approximately 10% of the photon energy. The longitudinal optical phonon scattering lifetime for electrons in the upper laser level is on the order of 5 ps and should only contribute ~2 meV of broadening to the transition, which is an order of magnitude smaller than what is seen in experiment. The significant portion of the transition broadening is thus from another source, and is frequently attributed to interface roughness scattering.[3–5] However, as seen in previous work,[6] the full width at half maximum (FWHM) of the optical transition ($2\gamma_{32}$) is both a function of current and temperature. Interface roughness scattering, however, should be largely independent of current density and temperature. Therefore, additional broadening mechanisms are contributing to the FWHM of the optical transition as a function of current density and temperature.

Possible sources of temperature and current dependent effects on the FWHM of the optical transition include band nonparabolicity in E-k space and a change in the alignment of minibands with changing field. Band nonparabolicity results in an increased transition width when more carriers are present or the carriers are distributed over a large range of k-space values (occurring at higher doping levels, temperature, and pump currents). The alignment of energy levels in the active region is primarily a function of injector barrier thickness, which has previously been used to control the FWHM of GaAs/AlGaAs QC structures.[7] For this experiment, we examine the optical transition width as a function of doping level, injector barrier thickness, current, and temperature in an effort to engineer the minimum of the FWHM at laser threshold, which does not necessarily occur in current QC structures.[6]

Four samples were grown back to back by molecular beam epitaxy with a similar conduction band structure to one reported previously,[8] an 8.2 μm QC laser, shown in Fig. 1. The four samples have varying injector doping levels and thickness of the injector barrier as described in Table I.

The devices consisted of 20 periods of active regions and injectors capped by 0.5 μm of GaInAs all lattice matched to InP. No waveguide layers were grown. The devices were fabricated as circular mesas, ~200 μm in diameter, with a top Ti/Au electrical contact and the bottom electrical contact made through the substrate. The samples were

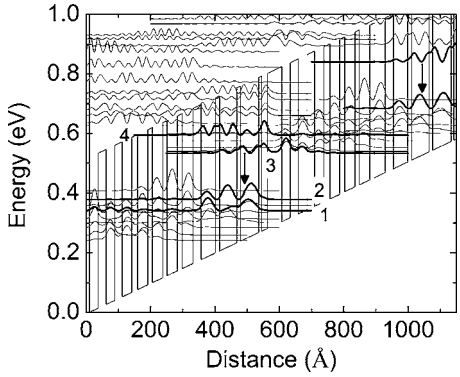

FIG. 1. Conduction band energy diagram for the samples in this study.

a)Electronic mail: showard@princeton.edu.

TABLE I. Sample number and corresponding doping level and injector barrier thickness.

	$n_{2D}=1\times10^{11}$ cm^{-2}	$n_{2D}=2\times10^{11}$ cm^{-2}
$t_{inject.barrier}=40$ Å	D322●	D3294◇
$t_{inject.barrier}=60$ Å	D3295■	D3295★

cleaved such that ~75% of the circular mesa remained with the cleaved facet as the edge emitter.

The voltage versus current characteristics of the samples were measured using 100 ns pulses at 3 kHz; the results are shown in Fig. 2(a). Stark-effect features ("steps" marked with an asterisk) present in the low doped samples indicate energy level misalignment at higher fields as described in previous work.[9] The low doped thin injection barrier sample also exhibits a high differential resistance region and indirect injection into the upper laser level via higher energy states. The increased differential resistance seen at ~6–7 V in the low doped samples could be controlled (and minimized) by a combination of injection barrier thickness and doping level of the injector. The devices all have a voltage turn on of ≤4 V. After turn on, the low doped samples have higher differential resistances than their higher doped counterparts. The devices exhibit lower differential resistance when the injection barrier is thinner for the same doping level. Overall, the best current transport (lowest differential resistance and avoiding Stark-effect voltage steps) occurs for the thin barrier high doped sample.

The electroluminescence (EL) spectra of the four samples are measured with a Thermo-Fisher Fourier transform infrared spectrometer in step scan mode while operating the device with ~1 μs pulses at 80 kHz repetition rate. First, the EL from a representative sample is analyzed to correlate the energy levels in the design to the measured optical transitions. Second, the four samples are compared first at the same temperature and pump current, and finally at the same temperature and different pump current densities.

The temperature dependent EL spectra of a representative sample from wafer D3294 are presented in Fig. 2(b). The fundamental transitions shift to lower energy with increasing temperature due to a decrease in the conduction band offset. The increase in the strength of the 1300 cm^{-1} with increasing temperature implies that it is thermally activated and is attributed to the 4→2 transition, which also agrees well with the transition calculated from the band structure. High temperatures (300 K) show transitions from electrons that were thermally excited into the continuum.

The EL spectra for different current densities and samples are presented in Figs. 2(c)–2(f). The thin barrier samples show nearly six times higher peak intensity than the thick barrier samples, indicating a larger number of carriers making the optical transition for the same current density. The fundamental (3→2) transition is clearly evident at ~1200 cm^{-1} as well as higher energy transitions at ~1350 cm^{-1} (4→2) and 1900 cm^{-1}. The higher energy transitions correspond to electron populations that do not contribute to the fundamental transition. Higher doped samples also show stronger 4→2 transitions than lower doped samples, indicating an increase in the number of electrons populating higher energy levels with an increase in doping. Additionally, thin barrier samples show a relatively stronger high energy→2 transition at 1900 cm^{-1} as electrons tunnel more easily into the continuum than in thick barrier structures. In agreement with previous work,[10] the luminescence wavelength of a 4 nm injection barrier does not depend on doping density, which is different from the dependence of the observed lasing wavelength on doping density in GaAs/AlGaAs structures.[11] The low doped thin

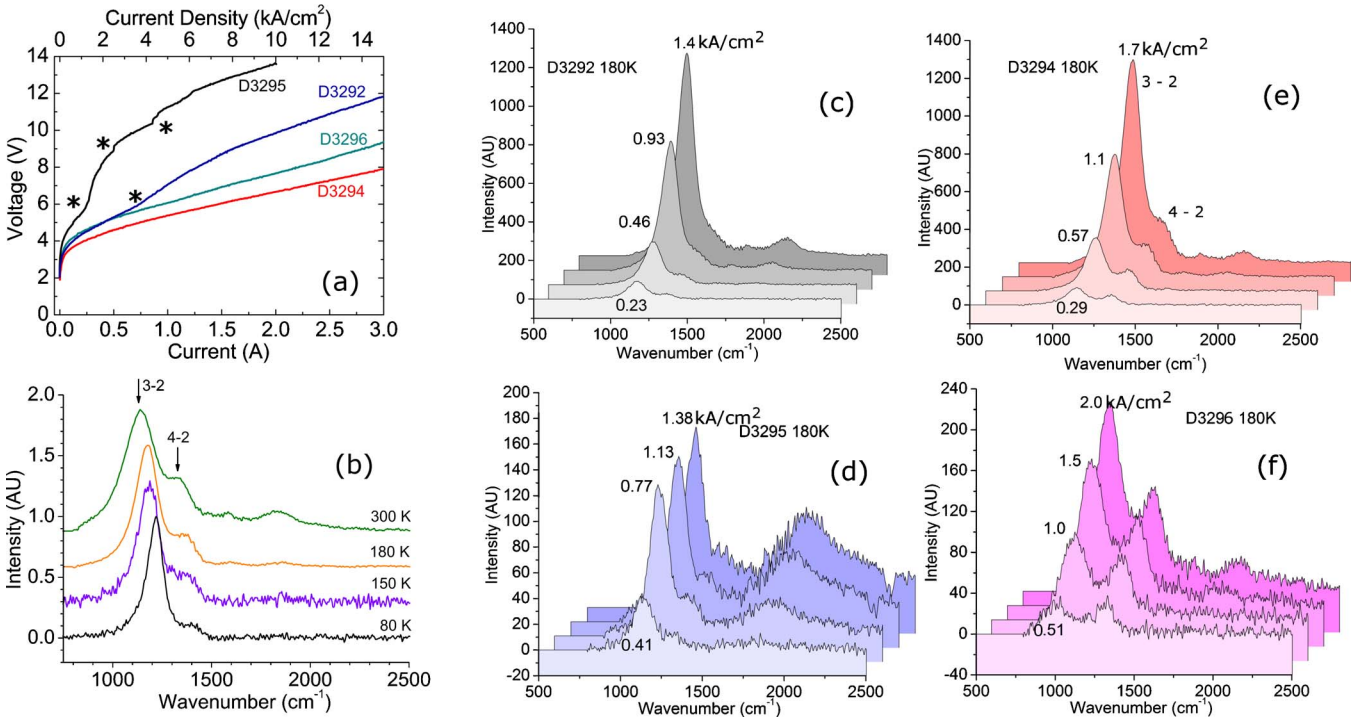

FIG. 2. (Color online) (a) Pulsed current-voltage characteristics at $T=80$ K for the four samples in the FWHM study. (b) EL spectra of D3294 as a function of temperature at a current density of 1 kA/cm^2. [(c)–(f)] EL spectra for different current densities at 180 K for all four samples.

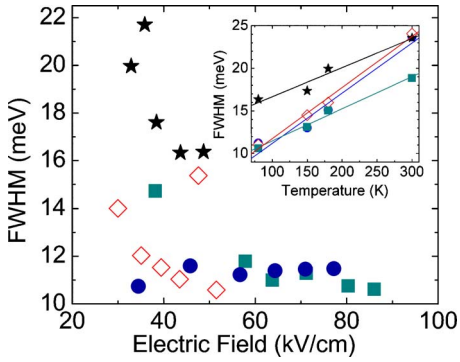

FIG. 3. (Color online) Minimum FWHM of the optical transition as a function of the applied electric field at $T=80$ K for the four samples in this study, as labeled in Table I. Inset: minimum FWHM of the optical transition as a function of temperature for the four samples in this study.

barrier sample has the smallest parasitic optical transitions with low injection into the continuum.

The FWHM of the transition versus temperature is summarized in Fig. 3 (inset). The thick injection barrier samples have a smaller (by a factor of 2) slope in FWHM versus temperature, and thus exhibit weaker temperature dependence of the transition width. In Fig. 3, low doped structures reach the minimum transition width faster than the high doped samples. In fact, D3292 achieves band alignment at fields lower than measured. Additionally, thin barrier structures exhibit the similar transition widths regardless of doping, in contrast to GaAs/AlGaAs QC structures[11] that exhibit a decrease in transition width with an increase in injection barrier thickness. In conclusion, thin injection barrier low doped structures have the best transition width (by ~20% compared to high doped thick barrier structures), luminescence intensity, and current transport prior to J_{max}.

The authors would like to acknowledge support from the MIRTHE-ERC and NSF-REU (NSF-ERC #EEC-0540832).

[1]J. Faist, D. Hofstetter, M. Beck, T. Aellen, M. Rochat, and S. Blaser, IEEE J. Quantum Electron. **38**, 533 (2002).
[2]M. Beck, D. Hofstetter, T. Aellen, J. Faist, U. Oesterle, M. Ilegems, E. Gini, and H. Melchior, Science **295**, 301 (2002).
[3]J. Faist, C. Sirtori, F. Capasso, L. Pfeiffer, and K. W. West, Appl. Phys. Lett. **64**, 872 (1994).
[4]S. Tsujino, A. Borak, E. Müller, M. Scheinert, C. V. Falub, H. Sigg, D. Grützmacher, M. Giovannini, and J. Faist, Appl. Phys. Lett. **86**, 062113 (2005).
[5]K. L. Campman, H. Schmidt, A. Imamoglu, and A. C. Gossard, Appl. Phys. Lett. **69**, 2554 (1996).
[6]S. S. Howard, Z. Liu, D. Wasserman, A. J. Hoffman, T. S. Ko, and C. F. Gmachl, IEEE J. Sel. Top. Quantum Electron. **13**, 1054 (2007).
[7]S. Barbieri, C. Sirtori, H. Page, M. Stellmacher, and J. Nagle, Appl. Phys. Lett. **78**, 282 (2001).
[8]Z. Liu, D. Wasserman, S. S. Howard, A. J. Hoffman, C. F. Gmachl, X. Wang, T. Tanbun-Ek, F. Choa, and L. Cheng, IEEE Photonics Technol. Lett. **18**, 1347 (2006).
[9]S. S. Howard, Z. Liu, and C. F. Gmachl, IEEE J. Quantum Electron. **44**, 319 (2008).
[10]T. Aellen, M. Beck, N. Hoyler, M. Giovannini, J. Faist, and E. Gini, J. Appl. Phys. **100**, 043101 (2006).
[11]M. Giehler, R. Hey, H. Kostial, S. Cronenberg, T. Ohtsuka, L. Schrottke, and H. T. Grahn, Appl. Phys. Lett. **82**, 671 (2003).